Supporting information

A Cationitrile Sequence Encodes Mild Poly(ionic liquid) Crosslinking for Advanced Composite Membranes

Zhiyue Dong[a], Chongrui Zhang[a], Huawen Peng[a], Jiang Gong[a], Hong Wang[b], Qiang Zhao[a],* and Jiayin Yuan[c]

Dr. Z. Dong, Dr. C. Zhang, Dr. H. Peng, Prof. J. Gong, Prof. Q. Zhao

a. Key Laboratory of Material Chemistry for Energy Conversion and Storage (Ministry of Education), Hubei Key Laboratory of Material Chemistry and Service Failure, School of Chemistry and Chemical Engineering, Huazhong University of Science and Technology, Wuhan 430074, China.

E-mail: zhaoq@hust.edu.cn (Q.Z.)

Prof. H. Wang

Key Laboratory of Functional Polymer Materials (Ministry of Education), Institute of Polymer Chemistry, College of Chemistry, Nankai University, Tianjin 300071, P. R. China

Prof. J.Y. Yuan

Department of Materials and Environmental Chemistry, Stockholm University, 10691 Stockholm, Sweden

Table of Contents

Section S1: Chemicals and characterizations

Chemicals and materials. 1-Vinylimidazole, bromoethane, bromopropionitrile, bromobutyronitrile and poly(4-vinylpyridine) were was purchase purchased from Aladdin Industrial Co (China). 1-Vinyl-3-benzyl imidazolium chlorine was purchased from Watson International Ltd, Suzhou, Jiangsu, China. 2-(1-Imidazolyl)acetonitrile was purchased from Lanzhou Kete Co. Ltd (China). Ammonium hydroxide (28 wt%), Congo red (CR), tetrahydrofuran (THF), dimethylsulfoxide (DMSO), N, N-dimethylformamide (DMF), EtOH, acetonitrile and N-methyl pyrrolidone (NMP) were all purchased from Sinopharm Chemical Reagent Co. Ltd (China). Glass substrates were purchased from Jiangsu Shitai Experimental Equipment Co. Ltd (China). Bis(trifluoromethane)sulfonimide lithium salt (Li-Tf_2N, 99%), sodium tetrafluoroborate ($NaBF_4$) and sodium hexafluorophosphate ($NaPF_6$) were purchased from Zhengzhou Alpha Chemical Co. Ltd (China). Azodiisobutyronitrile (AIBN) was purchased from Tianjing Fuchen Chemical Reagents Factory (China). Poly(vinylidene fluoride) (PVDF, diameter = 50 mm, pore size = 0.22 μm) membrane was bought from Shanghai Zuofei Experimental Equipment Co. Ltd (China). All the materials were analytical grade without further purification.

Characterizations. UV-Vis absorption spectra were performed with UV-Vis spectrophotometer (UV-6100 METASH). ^{1}H NMR (Nuclear Magnetic Resonance) spectra were conducted in Bruker Avance III 400MHz. Membrane morphologies and thickness were measured by atomic force microscope (AFM, SPM-9700, Shimadzu, tapping mode). ^{13}C CP-MAS NMR measurements were carried out on a 9.4 T wide-bore Bruker Avance III solid-state NMR spectrometer, operating at a Larmor frequency of 100.6 MHz. A 4.0 mm Bruker HX double resonance MAS probe was used. The NMR experiments were acquired at 25 °C and a MAS frequency of 10 kHz. X-ray photoelectron spectroscopy (XPS) of carbon element in nanomembrane was detected by ThrmoFisher Escalab 250XI. The Attenuated Total Reflect Fourier-Transform Infrared Spectroscopy (ATR FT-IR) images of polymers and membranes after NH_3 treatment were performed in Bruker VERTEX 70.

Section S2: **Synthesis of PCMVImTf_2N (P_3 polymer)[1-2]**

Synthesis of MVImBr monomer (Figure S1a). 1-Vinylimidazole (10 g) and bromoacetonitrile (15 g) were dissolved in 125 mL THF, heated in oil bath at 60 ^oC for 10 hours. The precipitates (MVImBr) were filtered, washed with THF for 3 times and vacuum dried at 50 ^oC for 12 hours. Yield: 70 % - 80 %.

Synthesis of PCMVImBr. MVImBr monomer (10 g) and AIBN imitator (80 mg) were dissolved in DMSO (100 mL), heated at 60 ^oC for 12 hours under nitrogen atmosphere. Afterwards the solution was dropped into excessive THF (1 L), and the precipitates (PCMVImBr) were collected, washed with THF three times and vacuum dried at 60 ^oC for overnight.

Preparation of PCMVImTf_2N (P_3) by counter ion exchange of PCMVImBr. 10 mL of LiTf_2N (1.4 g/mL) solution was added dropwise into PCMVImBr aqueous solution (20 mg/mL, 300 mL) under stirring (600 rpm). Then PCMVImTf_2N was collected as precipitates, washed by deionized water three times and vacuum dried at 50 ^oC for 16 hours.

Please note: PCMVIm-X (X denotes BF_4^-, PF_6^- counter ions) polymers were prepared by adding $NaBF_4$ and $NaPF_6$ aqueous solutions into PCMVIm-Br solution, respectively. PCMVIm-X was collected, purified and dried in the same method mentioned above.

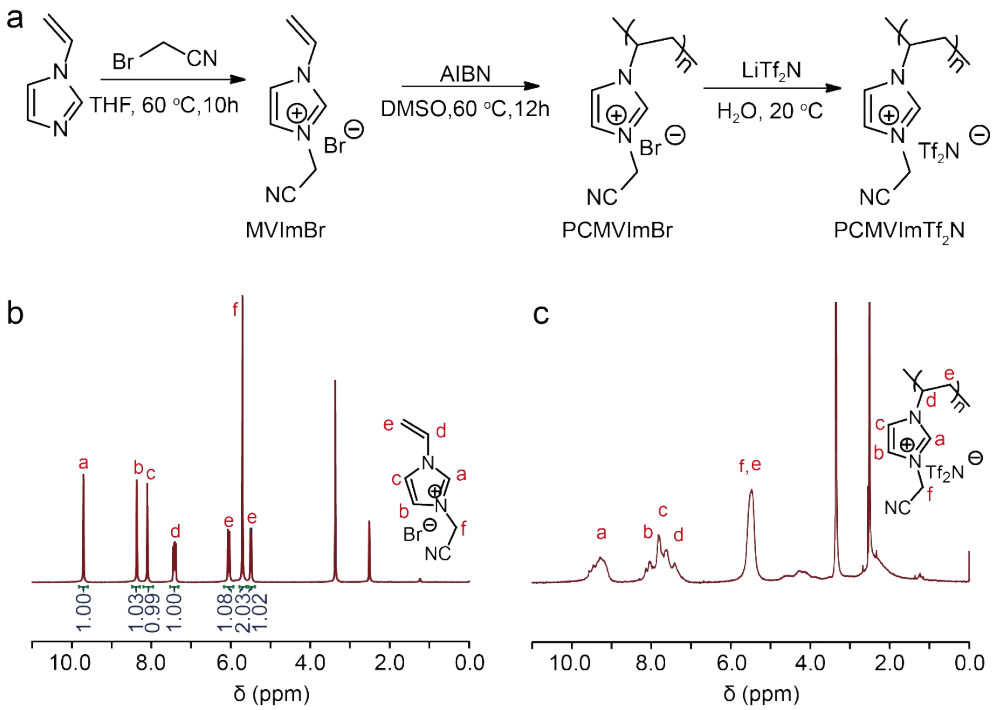

Figure S1. (a) Schematic synthesis of monomer (MVImBr) and polymer (PCMVImTf$_2$N, *P$_3$*) by radical polymerization and counter ion exchange. (b, c) ^{1}H NMR of MVImBr monomer and *P$_3$* polymer, respectively. Please note: For ^{1}H NMR, MVImBr (10 mg) and PCMVImTf$_2$N (50 mg) were dissolved in 600 μL methyl sulfoxide-d$_6$, respectively.

Section S3: **Membrane Preparation and Characterizations (thickness and stability in different solvents)**

Membrane preparation. PCMVImTf$_2$N was dissolved in DMF to prepare casting solution with different concentrations. 4 μL of polymer solution was casted on glass sheets (2 cm × 2 cm), dried at 80 ^{o}C for 2 hours. PCMVImTf$_2$N coating together with underlying glass slides were placed in NH_3 vapor (0.2 bar, 20 ^{o}C, 10 h), and then immersed into deionized water (20 ^{o}C). Free-standing membranes spontaneously peeled off from the glass slides. Please note: membranes from other polymers (P_1-P_7) were prepared by a similar method described above, if not otherwise specified.

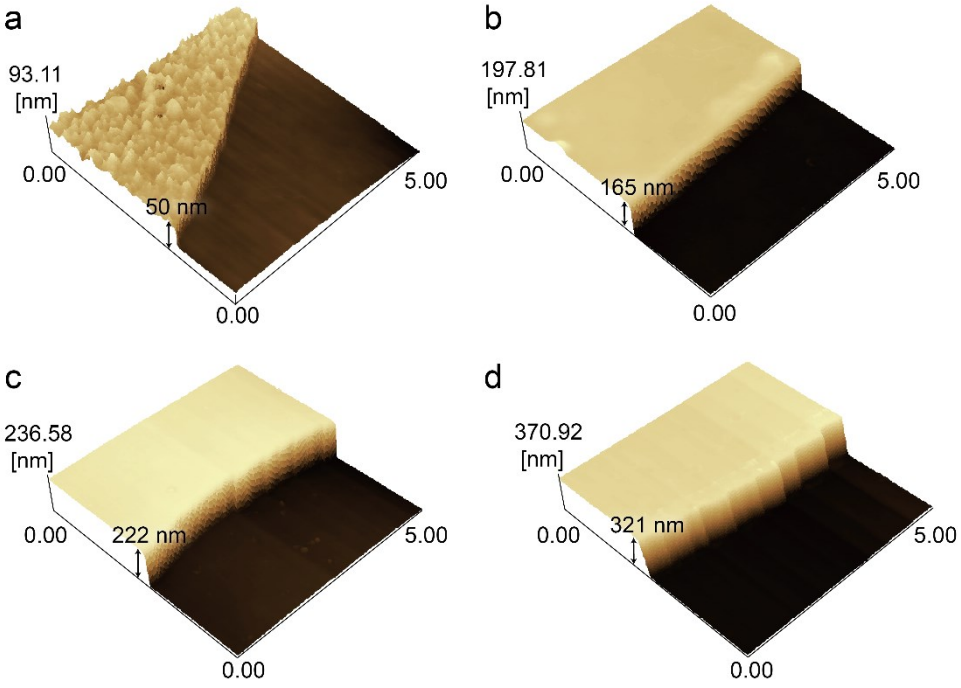

Figure S2. Thickness of freestanding membranes prepared from (a) 0.1 wt‰, (b) 0.2 wt‰, (c) 0.3 wt‰ and (d) 0.4 wt‰ of PCMVImTf$_2$N casting solution. Please note: thickness of P_3 nanomembrane prepared from 0.05 wt‰ PCMVImTf$_2$N casting solution was shown in Figure 1f (main text).

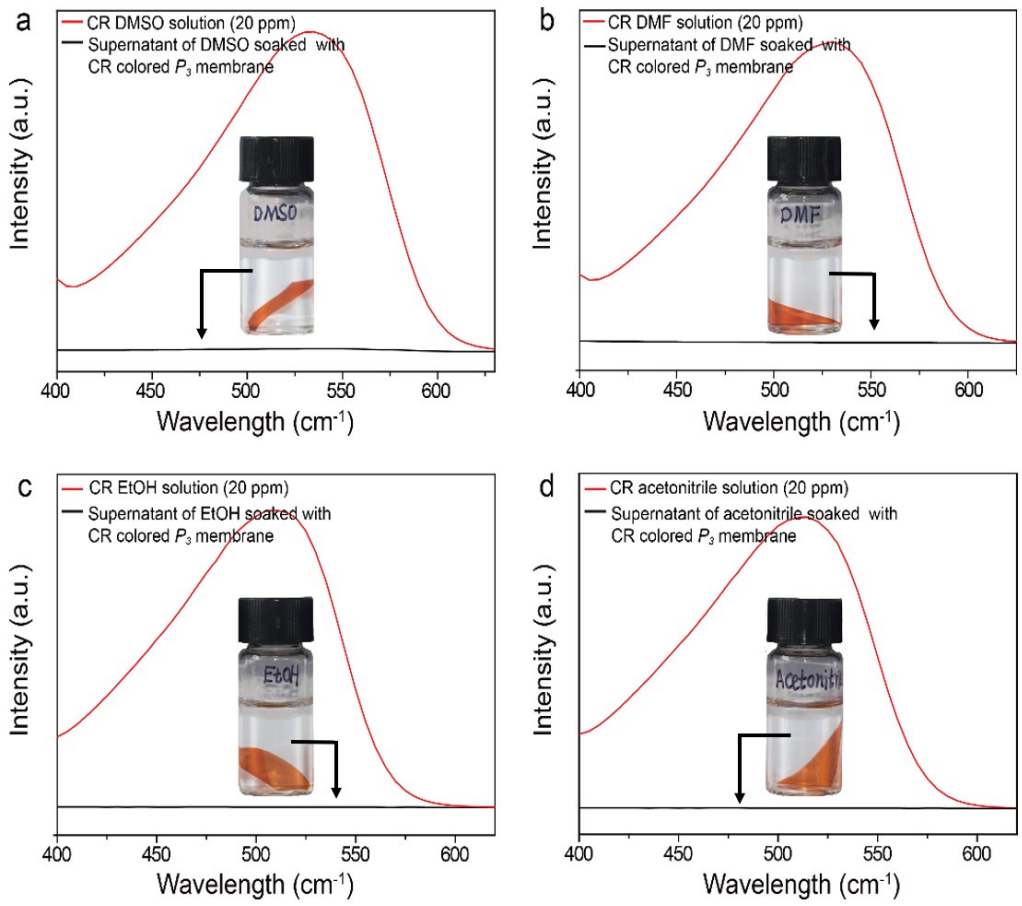

Figure S3. UV-Vis absorption (black line) of different supernatant solvents soaked with a piece of Congo red-containing P_3 nanomembrane: (a) DMSO; (b) DMF; (c) EtOH and (d) acetonitrile. Please note: UV-Vis absorption curves of Congo red solution (20 ppm, red line) in corresponding solvents were measured as comparison. The negligible Congo red absorbance in supernatant solvents indicates that the membranes was not excessively swelled in corresponding solvents, which is due to the crosslinking.

Section S4: Nanomembrane (P_3) characterizations (chemical structures)

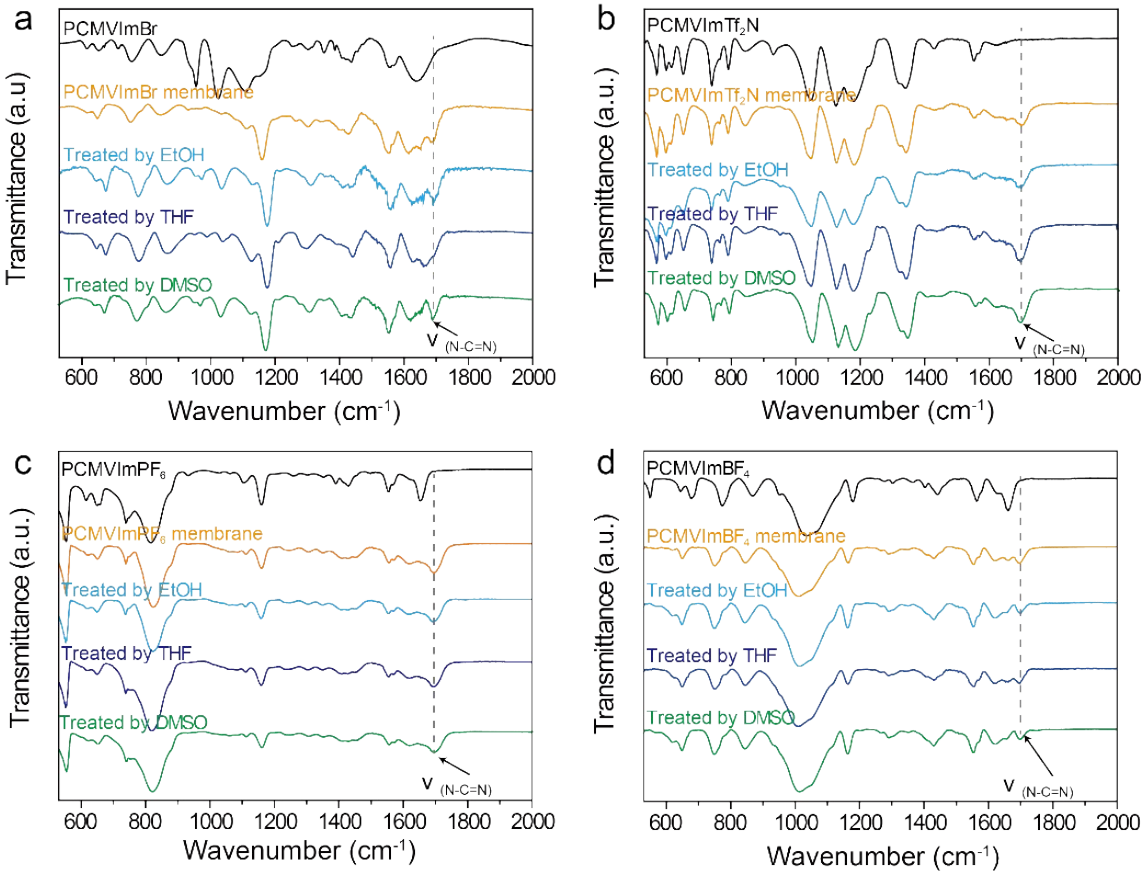

Figure S4. ATR FT-IR spectra of membranes made from (a) PCMVImBr, (b) $PCMVImTf_2N$, (c) $PCMVImPF_6$ and (d) $PCMVImBF_4$. Black curve: ATR FT-IR of pristine PCMVIm-X polymers; orange curve: ATR FT-IR of PCMVIm-X membranes; cyan, blue, green curves: ATR FT-IR of PCMVIm-X membranes after being soaked in EtOH, THF and DMSO solvents (25 ^{o}C, 24 h), respectively. Please note: X denotes different counter ions.

In Figure S4, a new peak around 1695 cm^{-1} revealed after NH_3 treatment (orange curve) of all PCMVIM-X membranes, which indicates the formation of triazine groups. This peak is maintained after treating the membranes with EtOH (cyan line), THF (blue line), DMSO (green line), indicating that the formed structure is stable.

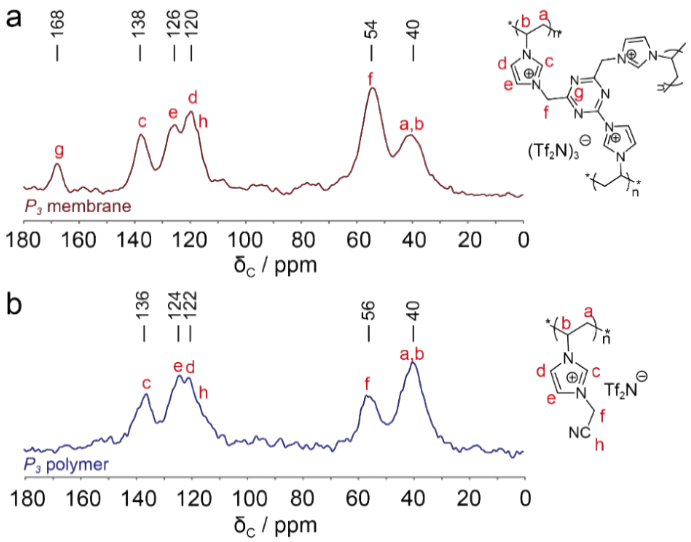

Figure S5. Solid-state ^{13}C NMR of (a) *P₃* nanomembrane and (b) pristine *P₃* polymer. Please note: a new peak (g) at chemical shift δ= 168 was seen, which is attributed to triazine ring formation in the nanomembrane.

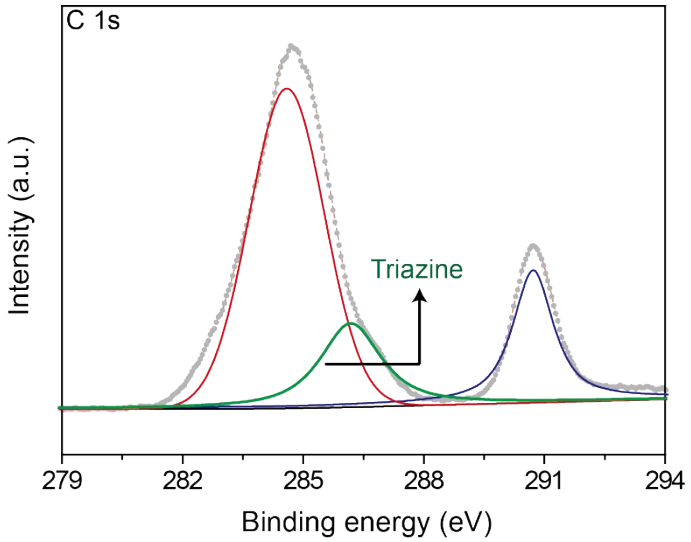

Figure S6. C 1s peaks of XPS profiles of *P₃* nanomembrane after NH_3 treatment. Please note: C 1s peak at 286.2 eV (green curve) belongs to carbon element in triazine ring, which also verifies the successful cyclization of nitrile groups to triazine ring by NH_3 vapor treatment[3].

***Section S5*: ATR FT-IR of different polymers (*P₁*-*P₂*, *P₄*-*P₇*) before and after NH_3 vapor treatment.**

Polymers *P₁*/*P₂*, *P₆*/*P₇*, *P₄*/*P₅* (Figure S7-S9, Figure 3, main text) were synthesized according to literatures[4-5].

(1) Synthesis of P_1 polymer (Figure S7a). 1-Vinylimidazole (5 g) and bromoethane (7.5 g) were dissolved in 125 mL THF, heated in oil bath at 60 °C for 10 hours. 1-Viny-3-ethylimidazole imidazole (VEImBr) monomer precipitates were filtered, washed with THF 3 times and dried in vacuum at 50 °C overnight. VEImBr (2 g) and AIBN initiator (20 mg) were dissolved in 50 mL DMSO, heated at 60 °C for 12 hours under nitrogen atmosphere. The final solution was dropped into excessive THF (500 mL), and the precipitates (P_1 polymer) were filtered, washed with THF 3 times and vacuum dried at 50 °C for 12 hours.

(2) Synthesis of P_2 polymer (Figure S7b). 1-Vinyl-3-benzyl imidazolium chlorine (VBImCl, 2 g) and AIBN initiator (20 mg) were dissolved in 50 mL DMSO, heated at 60 °C for 12 hours under nitrogen atmosphere. The final solution was dropped into excessive THF (500 mL) and the precipitates (P_2 polymer) were filtered, washed with THF 3 times and vacuum dried at 50 °C for 12 hours.

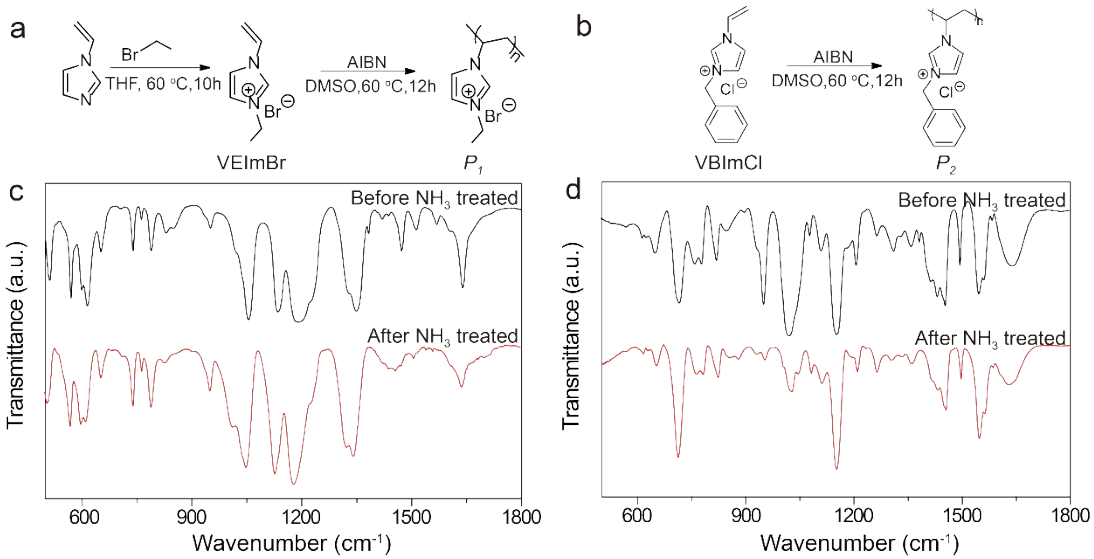

Figure S7. Synthesis schemes of polyelectrolyte polymer (a) P_1 and (b) P_2. ATR FT-IR spectra of (c) P_1 and (d) P_2 before and after being treated in NH_3 atmosphere. Please note: ATR FT-IR of P_1, P_2 polymers are identical before and after NH_3 vapor treatment. This indicates that no chemical reaction occurred during the NH_3 treatment.

(3) Synthesis of P_6 polymer. 1-Vinylimidazole (2 g) and bromopropionitrile (3 g) were dissolved in 50 mL THF, heated in oil bath at 55 °C for 14 hours. 1-Viny-3-nitrilepropyl imidazole (VNPImBr) monomer was produced as precipitates, which were

filtered, washed with THF 3 times and dried in vacuum at 50 °C for overnight. VNPImBr (1 g) and AIBN initiator (10 mg) were dissolved in 30 mL DMSO, heated at 70 °C for 16 hours under nitrogen atmosphere. The final solution was dropped into excessive THF (300 mL), and the precipitates (P_6 polymer) were filtered, washed with THF 3 times and vacuum dried at 50 °C for 12 hours.

(4) Synthesis of P_7 polymer. 1-Vinylimidazole (2 g) and bromobutyronitrile (3 g) were dissolved in 50 mL THF, heated in oil bath at 55 °C for 14 hours. 1-Viny-3-nitrilebutyl imidazole (VNBImBr) monomer was produced as precipitates, which were filtered, washed with THF 3 times and dried in vacuum at 50 °C for overnight. VNBImBr (1 g) and AIBN initiator (10 mg) were dissolved in 30 mL DMSO, heated at 70 °C for 16 hours under nitrogen atmosphere. The final solution was dropped into excessive THF (300 mL), and the precipitates (P_7 polymer) were filtered, washed with THF 3 times and vacuum dried at 50 °C for 12 hours.

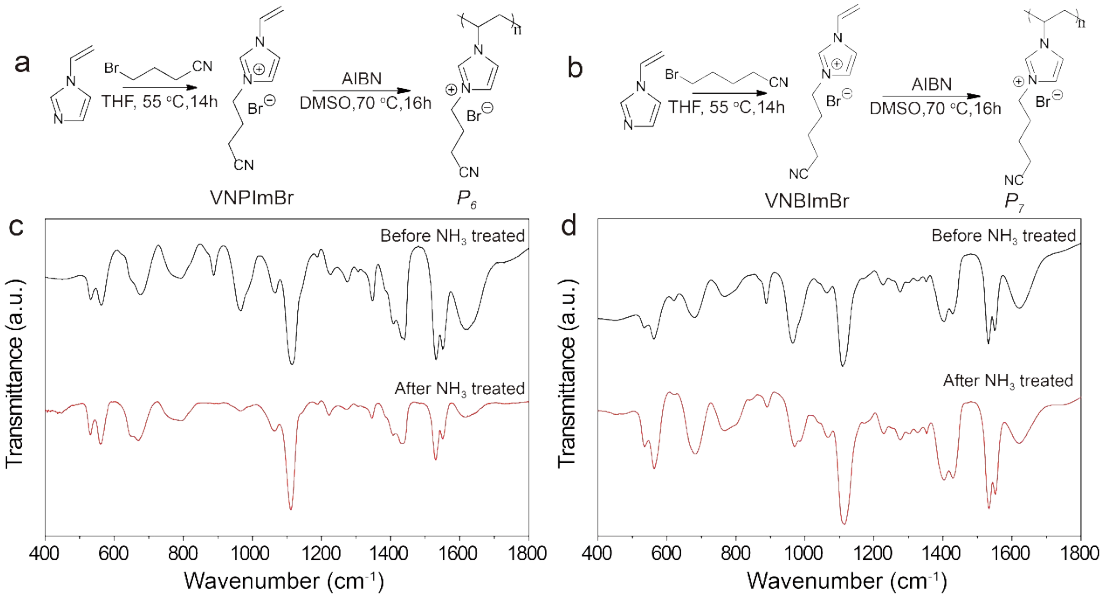

Figure S8. (a, b) Synthesis of P_6 and P_7 polymer, respectively. (c, d) ATR FT-IR spectra of P_6 andP_7 before and after being treated in NH_3 atmosphere, respectively. Please note: ATR FT-IR of P_6, P_7 polymers are identical before and after NH_3 vapor treatment. This indicates that no chemical reaction occurred during the NH_3 treatment.

(5) Synthesis of P_4 polymer. Poly(4-vinylpyridine) (PVP, MW: 2000, 2 g) and bromoacetonitrile (3 g) were dissolved in 100 mL NMP, heated in oil bath at 70 °C for

3 days. The precipitates (P_4) were vacuum filtered, washed with THF 3 times and dried in vacuum at 50 °C for overnight.

(6) Synthesis of P_5 polymer. 1-Vinytriazole (12 g), bromoacetonitrile (3.78 g) and 2,6-di-tert-butyl-4-methylphenol stabilizer (18 mg) were dissolved in 30 mL THF, heated at 55 °C for 3 days. 1-Vinyl-3-cyanomethyl imidazolium bromide (CMVTBr) monomer was produced as precipitates, which were vacuum filtered, washed with diethyl ether 3 times and dried in vacuum at 50 °C for overnight. CMVTBr (3 g) and AIBN initiator (10 mg) were dissolved in 30 mL DMSO, heated at 70 °C for 16 hours under nitrogen atmosphere. The final solution was dropped into excessive THF (300 mL), and the precipitates (P_5 polymer) were filtered, washed with THF 3 times and vacuum dried at 50 °C for 12 hours.

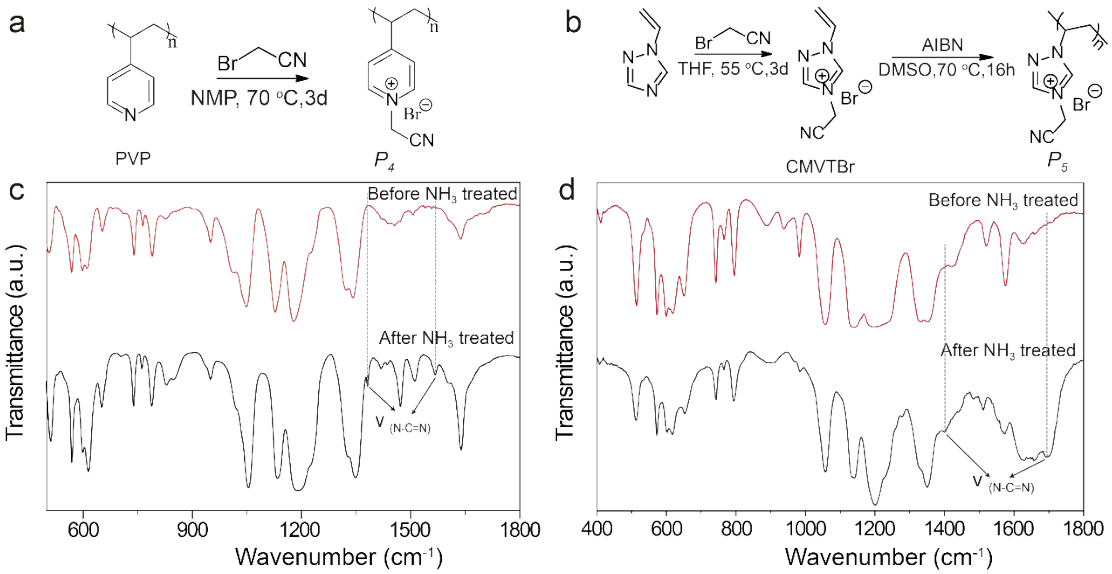

Figure S9. (a, b) Synthesis schemes P_4 and P_5 polymer, respectively. (c, d) ATR FT-IR spectra of P_4 and P_5 before and after being treated in NH_3 atmosphere. Please note: Compared to pristine polymers (red lines), new peaks at 1383 cm^{-1} and 1573 cm^{-1} (black line) in P_4 and new peaks at 1401cm^{-1} and 1695 cm^{-1} (black line) in P_5 were seen after NH_3 vapor treatment.

Section S6: Solvent stability of membranes (P_1-P_7) treated by ammonia vapor

Congo red dye was added into different casting solution of different polymers (P_1-P_7) to prepare colored membranes, which were all treated in ammonia vapor (0.2 bar, 14 h, 20 °C). The membranes made from P_4 and P_5 polymer remain insoluble with good

integrity (Figure S10), due to the "polycationitrile" crosslinking (Figure S9). By contrast, polymer membranes (P_1, P_2, P_6, P_7) dissolved in DMSO solvent, because these polymers could not undergo "polycationitrile" crosslinking (Figure S7, Figure S8).

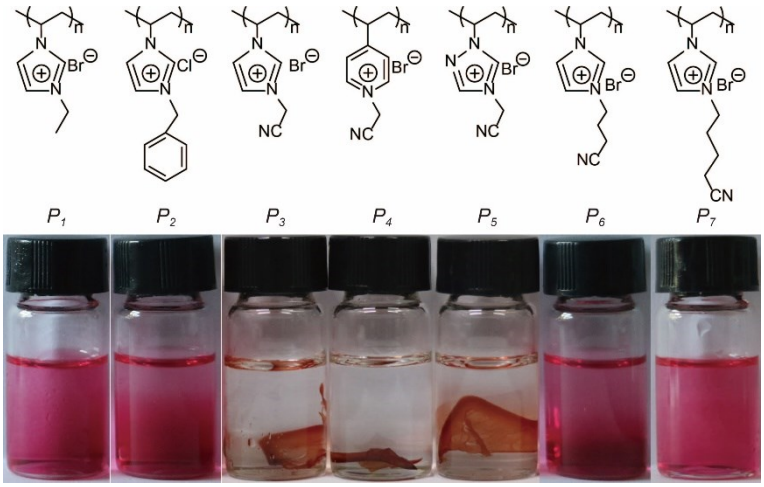

Figure S10. Stability of different polymer membranes immersed in DMSO (25 °C, 24 h). Please note: These membranes were all treated with ammonia vapor (0.2 bar, 14 h, 20 °C).

Section S7: Fabrication of PCMVImTf$_2$N/CNT/UiO-66-COOH hybrid membrane and property of solar steam evaporation

Fabrication of the PCMVImTf$_2$N/CNT/UiO-66-COOH hybrid membrane: UiO-66-COOH (20 mg) and CNTs (3.2 mg) were dispersed in 20 ml of PCMVImTf$_2$N DMF (0.43 mg/mL) by stirring and ultrasound. Then the dispersion was filtrated onto PVDF substrate membrane, treated in NH_3 vapor (0.2 bar, 14 h, 20 °C). Finally, the PCMVImTf$_2$N/CNT/UiO-66-COOH membrane was utilized for solar steam evaporation under one sunlight (1kW·m^{-2}) irradiation.

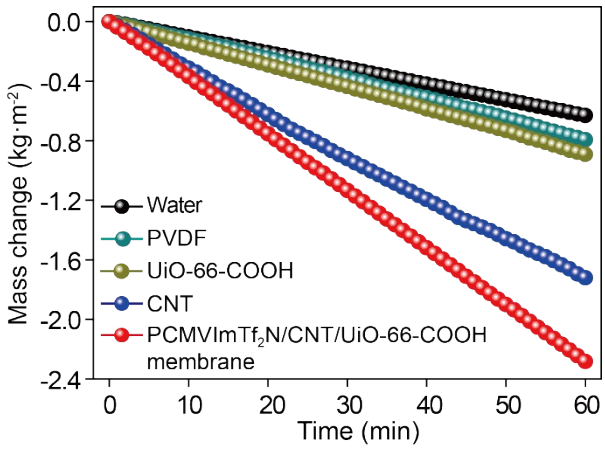

Figure S11. Mass loss of water under 1kW·m^{-2} irradiation on different materials.

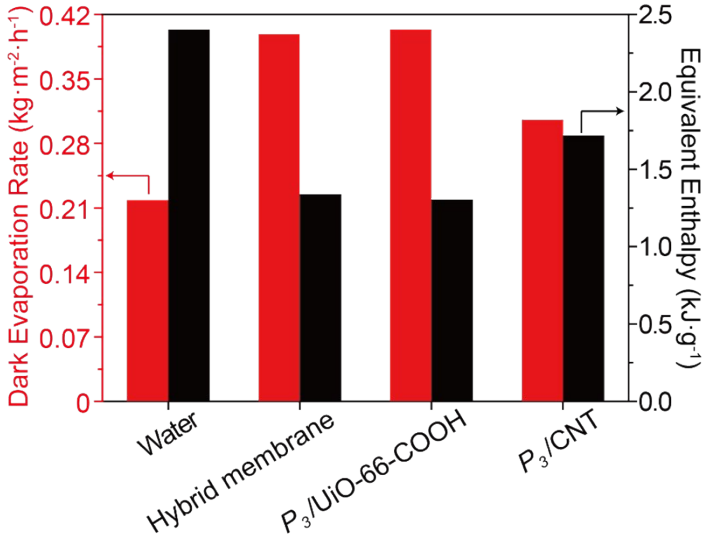

Figure S12. Enthalpy values of different materials (black columns) calculated from the water evaporation rate in dark (red columns). Please note: the calculation is based on $Q_m = Q_w(E_w/E_m)$. In this equation, Q_m is the evaporation enthalpy of water in hybrid membrane, Q_w is the evaporation enthalpy of bulk water, E_w is the dark evaporation rate of bulk water and E_m is the water evaporation rate of hybrid membrane in dark). The enthalpy values of bulk water, hybrid membrane, P_3/UiO-66-COOH and P_3/CNT are 2.4 kJ·g^{-1}, 1.33 kJ·g^{-1}, 1.3 kJ·g^{-1} and 1.7 kJ·g^{-1}, respectively.

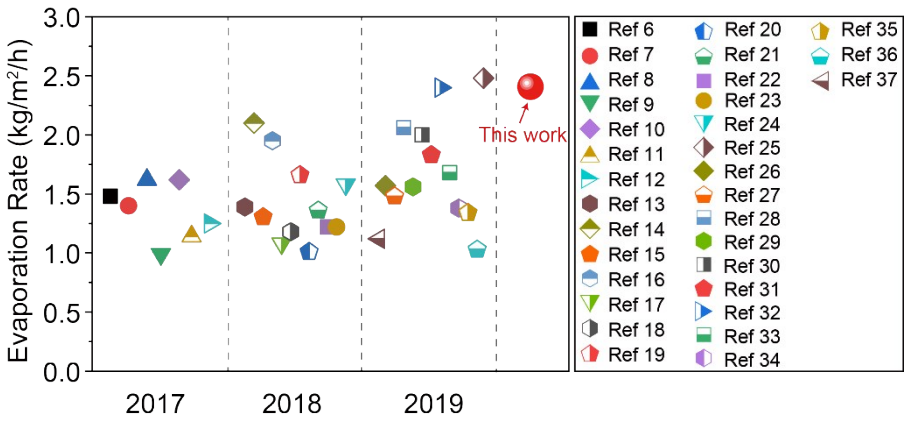

Figure S13. Solar steam performance (under one sun irradiation) of PCMVImTf$_2$N/CNT/UiO-66-COOH membrane in this work compared with state-of-the-art carbon-based materials in 2017-2019[6-37]. Refs 6-37 were listed at the end of the supporting information.

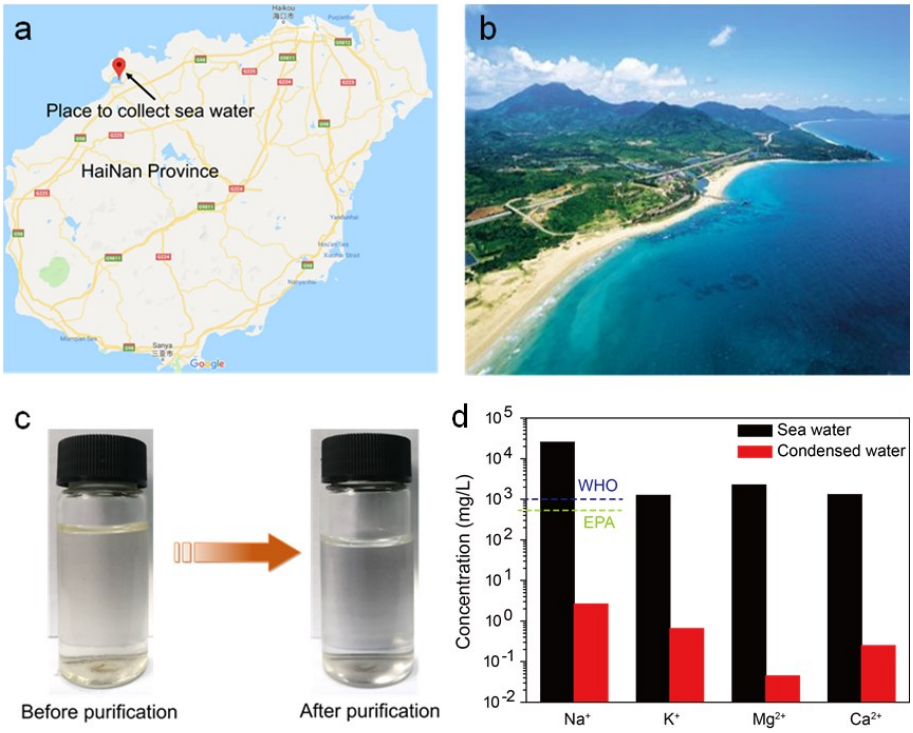

Figure S14 (a, b) Detailed location where the seawater was collected (South Sea China). (c) Images of seawater before and after being treated by solar thermal desalination using PCMVImTf$_2$N/CNT/UiO-66-COOH hybrid membrane. The seawater after purification is clear and transparent. (d) Ions concentration of seawater and condensed water after solar desalination.

REFERENCES

1. Gao, Y.; Gao, H.; Piekarski, C.; Shreeve, J. n. M., Azolium Salts Functionalized with Cyanomethyl, Vinyl, or Propargyl Substituents and Dicyanamide, Dinitramide, Perchlorate and Nitrate Anions. *European Journal of Inorganic Chemistry* **2007,** *2007* (31), 4965-4972.
2. Koebe, M.; Drechsler, M.; Weber, J.; Yuan, J., Crosslinked poly(ionic liquid) nanoparticles: inner structure, size, and morphology. *Macromolecular rapid communications* **2012,** *33* (8), 646-51.
3. Zhou, T.; Zhao, Y.; Choi, J. W.; Coskun, A., Lithium-Salt Mediated Synthesis of a Covalent Triazine Framework for Highly Stable Lithium Metal Batteries. *Angewandte Chemie* **2019,** *58* (47), 16795-16799.
4. Zhang, W.; Willa, C.; Sun, J.-K.; Guterman, R.; Taubert, A.; Yuan, J., Polytriazolium poly(ionic liquid) bearing triiodide anions: Synthesis, basic properties and electrochemical behaviors. *Polymer* **2017,** *124*, 246-251.
5. Yuan, J.; Giordano, C.; Antonietti, M., Ionic Liquid Monomers and Polymers as Precursors of Highly Conductive, Mesoporous, Graphitic Carbon Nanostructures. *Chemistry of Materials* **2010,** *22* (17), 5003-5012.
6. Xu, N.; Hu, X.; Xu, W.; Li, X.; Zhou, L.; Zhu, S.; Zhu, J., Mushrooms as Efficient Solar Steam-Generation Devices. *Advanced materials* **2017,** *29* (28).
7. Ren, H.; Tang, M.; Guan, B.; Wang, K.; Yang, J.; Wang, F.; Wang, M.; Shan, J.; Chen, Z.; Wei, D.; Peng, H.; Liu, Z., Hierarchical Graphene Foam for Efficient Omnidirectional Solar-Thermal Energy Conversion. *Advanced materials* **2017,** *29* (38).
8. Hu, X.; Xu, W.; Zhou, L.; Tan, Y.; Wang, Y.; Zhu, S.; Zhu, J., Tailoring Graphene Oxide-Based Aerogels for Efficient Solar Steam Generation under One Sun. *Advanced materials* **2017,** *29* (5).
9. Chen, C.; Li, Y.; Song, J.; Yang, Z.; Kuang, Y.; Hitz, E.; Jia, C.; Gong, A.; Jiang, F.; Zhu, J. Y.; Yang, B.; Xie, J.; Hu, L., Highly Flexible and Efficient Solar Steam Generation Device. *Advanced materials* **2017,** *29* (30).
10. Zhang, P.; Li, J.; Lv, L.; Zhao, Y.; Qu, L., Vertically Aligned Graphene Sheets Membrane for Highly Efficient Solar Thermal Generation of Clean Water. *ACS nano* **2017,** *11* (5), 5087-5093.
11. Guo, A.; Ming, X.; Fu, Y.; Wang, G.; Wang, X., Fiber-Based, Double-Sided, Reduced Graphene Oxide Films for Efficient Solar Vapor Generation. *ACS applied materials & interfaces* **2017,** *9* (35), 29958-29964.
12. Li, Y.; Gao, T.; Yang, Z.; Chen, C.; Luo, W.; Song, J.; Hitz, E.; Jia, C.; Zhou, Y.; Liu, B.; Yang, B.; Hu, L., 3D-Printed, All-in-One Evaporator for High-Efficiency Solar Steam Generation under 1 Sun Illumination. *Advanced materials* **2017,** *29* (26).
13. Zhu, L.; Gao, M.; Peh, C. K. N.; Wang, X.; Ho, G. W., Self-Contained Monolithic Carbon Sponges for Solar-Driven Interfacial Water Evaporation Distillation and Electricity Generation. *Advanced Energy Materials* **2018,** *8* (16), 1702149.
14. Zhang, P.; Liao, Q.; Yao, H.; Cheng, H.; Huang, Y.; Yang, C.; Jiang, L.; Qu, L., Three-dimensional water evaporation on a macroporous vertically aligned graphene pillar array under one sun. *Journal of Materials Chemistry A* **2018,** *6* (31), 15303-15309.
15. Yang, Y.; Zhao, R.; Zhang, T.; Zhao, K.; Xiao, P.; Ma, Y.; Ajayan, P. M.; Shi, G.; Chen, Y., Graphene-Based Standalone Solar Energy Converter for Water Desalination and Purification. *ACS nano* **2018,** *12* (1), 829-835.
16. Li, W.; Tekell, M. C.; Huang, Y.; Bertelsmann, K.; Lau, M.; Fan, D., Synergistic High-Rate Solar Steaming and Mercury Removal with MoS2

/C @ Polyurethane Composite Sponges. *Advanced Energy Materials* **2018,** *8* (32), 1802108.
17. Liu, H.; Chen, C.; Chen, G.; Kuang, Y.; Zhao, X.; Song, J.; Jia, C.; Xu, X.; Hitz, E.; Xie, H.; Wang, S.; Jiang, F.; Li, T.; Li, Y.; Gong, A.; Yang, R.; Das, S.; Hu, L., High-Performance Solar Steam Device with Layered Channels: Artificial Tree with a Reversed Design. *Advanced Energy Materials* **2018,** *8* (8), 1701616.
18. Li, T.; Liu, H.; Zhao, X.; Chen, G.; Dai, J.; Pastel, G.; Jia, C.; Chen, C.; Hitz, E.; Siddhartha, D.; Yang, R.; Hu, L., Scalable and Highly Efficient Mesoporous Wood-Based Solar Steam Generation Device: Localized Heat, Rapid Water Transport. *Advanced Functional Materials* **2018,** *28* (16), 1707134.
19. Zhang, P.; Liu, F.; Liao, Q.; Yao, H.; Geng, H.; Cheng, H.; Li, C.; Qu, L., A Microstructured Graphene/Poly(N-isopropylacrylamide) Membrane for Intelligent Solar Water Evaporation. *Angewandte Chemie* **2018,** *57* (50), 16343-16347.
20. Gao, M.; Peh, C. K.; Phan, H. T.; Zhu, L.; Ho, G. W., Solar Absorber Gel: Localized Macro-Nano Heat Channeling for Efficient Plasmonic Au Nanoflowers Photothermic Vaporization and Triboelectric Generation. *Advanced Energy Materials* **2018,** *8* (25), 1800711.
21. Wang, Y.; Wang, C.; Song, X.; Megarajan, S. K.; Jiang, H., A facile nanocomposite strategy to fabricate a rGO–MWCNT photothermal layer for efficient water evaporation. *Journal of Materials Chemistry A* **2018,** *6* (3), 963-971.
22. Shao, Y.; Jiang, Z.; Zhang, Y.; Wang, T.; Zhao, P.; Zhang, Z.; Yuan, J.; Wang, H., All-Poly(ionic liquid) Membrane-Derived Porous Carbon Membranes: Scalable Synthesis and Application for Photothermal Conversion in Seawater Desalination. *ACS nano* **2018,** *12* (11), 11704-11710.
23. Li, H.; He, Y.; Hu, Y.; Wang, X., Commercially Available Activated Carbon Fiber Felt Enables Efficient Solar Steam Generation. *ACS applied materials & interfaces* **2018,** *10* (11), 9362-9368.
24. Liu, F.; Zhao, B.; Wu, W.; Yang, H.; Ning, Y.; Lai, Y.; Bradley, R., Low Cost, Robust, Environmentally Friendly Geopolymer-Mesoporous Carbon Composites for Efficient Solar Powered Steam Generation. *Advanced Functional Materials* **2018,** *28* (47), 1803266.
25. Sun, Z.; Li, W.; Song, W.; Zhang, L. c.; Wang, Z., High-efficiency Solar Desalination Evaporator Composite of Corn Stalk, Mcnt and TiO2: Ultra-fast Capillary Water Moisture Transportation and Porous Bio-tissues Multi-layers Filtration. *Journal of Materials Chemistry A* **2019**.
26. Liu, J.; Liu, Q.; Ma, D.; Yuan, Y.; Yao, J.; Zhang, W.; Su, H.; Su, Y.; Gu, J.; Zhang, D., Simultaneously achieving thermal insulation and rapid water transport in sugarcane stems for efficient solar steam generation. *Journal of Materials Chemistry A* **2019,** *7* (15), 9034-9039.
27. Xia, Y.; Hou, Q.; Jubaer, H.; Li, Y.; Kang, Y.; Yuan, S.; Liu, H.; Woo, M. W.; Zhang, L.; Gao, L.; Wang, H.; Zhang, X., Spatially isolating salt crystallisation from water evaporation for continuous solar steam generation and salt harvesting. *Energy & Environmental Science* **2019,** *12* (6), 1840-1847.
28. Hu, G.; Cao, Y.; Huang, M.; Wu, Q.; Zhang, K.; Lai, X.; Tu, J.; Tian, C.; Liu, J.; Huang, W.; Ding, L., Salt-Resistant Carbon Nanotubes/Polyvinyl Alcohol Hybrid Gels with Tunable Water Transport for High-Efficiency and Long-Term Solar Steam Generation. *Energy Technology* **2019**, 1900721.
29. Yu, Z.; Cheng, S.; Li, C.; Li, L.; Yang, J., Highly Efficient Solar Vapor Generator Enabled by a 3D Hierarchical Structure Constructed with Hydrophilic Carbon Felt for Desalination and Wastewater Treatment. *ACS applied materials & interfaces* **2019,** *11* (35), 32038-32045.
30. Xu, W.; Xing, Y.; Liu, J.; Wu, H.; Cui, Y.; Li, D.; Guo, D.; Li, C.; Liu, A.; Bai, H., Efficient Water Transport and Solar Steam Generation via Radially, Hierarchically Structured Aerogels. *ACS nano* **2019,** *13* (7), 7930-7938.

31. Tan, M.; Wang, J.; Song, W.; Fang, J.; Zhang, X., Self-floating hybrid hydrogels assembled with conducting polymer hollow spheres and silica aerogel microparticles for solar steam generation. *Journal of Materials Chemistry A* **2019,** *7* (3), 1244-1251.
32. Hanxue Liang, Q. L., Nan Chen, Yuan Liang, Guiqin Lv, Panpan Zhang, Bing Lu, Liangti Qu, Thermal efficiency of solar steam generation approaching 100% through capillary water transport. *Angew Chem Int Ed* **2019**.
33. Zhang, B.; Song, C.; Liu, C.; Min, J.; Azadmanjiri, J.; Ni, Y.; Niu, R.; Gong, J.; Zhao, Q.; Tang, T., Molten salts promoting the "controlled carbonization" of waste polyesters into hierarchically porous carbon for high-performance solar steam evaporation. *Journal of Materials Chemistry A* **2019,** *7* (40), 22912-22923.
34. Ma, X.; Fang, W.; Guo, Y.; Li, Z.; Chen, D.; Ying, W.; Xu, Z.; Gao, C.; Peng, X., Hierarchical Porous SWCNT Stringed Carbon Polyhedrons and PSS Threaded MOF Bilayer Membrane for Efficient Solar Vapor Generation. *Small* **2019**, e1900354.
35. Qin, D.-D.; Zhu, Y.-J.; Chen, F.-F.; Yang, R.-L.; Xiong, Z.-C., Self-floating aerogel composed of carbon nanotubes and ultralong hydroxyapatite nanowires for highly efficient solar energy-assisted water purification. *Carbon* **2019,** *150*, 233-243.
36. Qiu, P.; Liu, F.; Xu, C.; Chen, H.; Jiang, F.; Li, Y.; Guo, Z., Porous three-dimensional carbon foams with interconnected microchannels for high-efficiency solar-to-vapor conversion and desalination. *Journal of Materials Chemistry A* **2019,** *7* (21), 13036-13042.
37. Liu, S.; Huang, C.; Huang, Q.; Wang, F.; Guo, C., A new carbon-black/cellulose-sponge system with water supplied by injection for enhancing solar vapor generation. *Journal of Materials Chemistry A* **2019,** *7* (30), 17954-17965.